J|A|C|S
ARTICLES
Published on Web 06/12/2003

Mechanism for the Noncovalent Chiral Domino Effect: New Paradigm for the Chiral Role of the N-Terminal Segment in a 3_{10}-Helix

Yoshihito Inai,* Naoki Ousaka, and Takahiro Okabe

Contribution from the Department of Environmental Technology and Urban Planning, Graduate School of Engineering, Nagoya Institute of Technology, Gokiso-cho, Showa-ku, Nagoya 466-8555, Japan

Received March 7, 2003; E-mail: inai@mse.nitech.ac.jp

Abstract: Recently, novel chiral interactions on 3_{10}-helical peptides, of which the helicity is controlled by external chiral stimulus operating on the N-terminus, were proposed as a "noncovalent chiral domino effect (NCDE)" (Inai, Y.; et al. *J. Am. Chem. Soc.* **2000**, *122*, 11731. Inai, Y.; et al. *J. Am. Chem. Soc.* **2002**, *124*, 2466). The present study clarifies the mechanism for generating the NCDE. For this purpose, achiral nonapeptide (**1**), H-β-Ala-(Δ^ZPhe-Aib)$_4$-OMe [Δ^ZPhe = (*Z*)-didehydrophenylalanine, Aib = α-aminoisobutyric acid], was synthesized. Peptide **1** alone adopts a 3_{10}-helical conformation in chloroform. On the basis of the induced CD signals of peptide **1** with chiral additives, chiral acid enabling the predominant formation of a one-handed helix was shown to need at least both carboxyl and urethane groups; that is, Boc-L-amino acid (Boc = *tert*-butoxycarbonyl) strongly induces a right-handed helix. NMR studies (NH resonance variations, low-temperature measurement, and NOESY) were performed for a $CDCl_3$ solution of peptide **1** and chiral additive, supporting the view that the N-terminal H-β-Ala-Δ^ZPhe-Aib, including the two free amide NH's, captures effectively a Boc-amino acid molecule through three-point interactions. The H-β-Ala's amino group binds to the carboxyl group to form a salt bridge, while the Aib(3) NH is hydrogen-bonded to either oxygen of the carboxylate group. Subsequently, the free Δ^ZPhe(2) NH forms a hydrogen bond to the urethane carbonyl oxygen. A semiempirical molecular orbital computation explicitly demonstrated that the dynamic looping complexation is energetically permitted and that the N-terminal segment of a right-handed 3_{10}-helix binds more favorably to a Boc-L-amino acid than to the corresponding D-species. In conclusion, the N-terminal segment of a 3_{10}-helix, ubiquitous in natural proteins and peptides, possesses the potency of chiral recognition in the backbone itself, furthermore enabling the conversion of the terminally acquired chiral sign and power into a dynamic control of the original helicity and helical stability.

Introduction

A helix is the most ubiquitous macrochiral structure for natural macromolecules (protein, DNA, and polysaccharide), serving as a fundamental building block for constructing elaborate architectures leading to versatile biological processes. Noncovalent chiral interactions operating on a biological helix thus would affect largely the structural feature and stability of ternary structures, thereby altering the original activities and functionalities. Chiral recognition in living systems has been mainly focused on the binding manner of a small chiral guest in a biological macromolecule. Conversely, the importance of chiral interactions influencing a biological helix (helicity or stability) is ill-defined. The difficulty is based on the complexity of biological systems that bring about many types of simultaneous interactions to prevent us from highlighting only chiral factors. In addition, the coexistence of nonhelical conformations, frequently accompanied with a biological helix, renders the alternative problem (left-handed or right-handed helicity) more ambiguous.

Correspondingly, many scientists have been producing model systems to facilitate the understanding of such chiral effects on a helical structure. There have already been reported a surprising number of elegant artificial helical backbones and supramolecular systems to elucidate covalent (static) and noncovalent (dynamic) induction of a one-handed helix through small chiral molecules.[1] Recently, particular attention has been paid to the helical screw-sense induction of an optically inactive chain through external chiral stimulus (additive agent, solvent, light, and so on).[2−6] For instance, an achiral synthetic polymer bearing functional groups in the repeating monomer unit interacts with added chiral small molecules on its polymer side chain or main chain, in turn leading to the predominant formation of a one-handed helix.[2]

These chiral inductions originate from side-chain or main-chain interactions on an achiral chain. In contrast, we have found

(1) (a) Nolte, R. J. M. *Chem. Soc. Rev.* **1994**, *23*, 11−19. (b) Nakano, T.; Okamoto, Y. *Chem. Rev.* **2001**, *101*, 4013−4038. (c) Hill, D. J.; Mio, M. J.; Prince, R. B.; Hughes, T. S.; Moore, J. S. *Chem. Rev.* **2001**, *101*, 3893−4011. (d) Brunsveld, L.; Folmer, B. J. B.; Meijer, E. W.; Sijbesma, R. P. *Chem. Rev.* **2001**, *101*, 4071−4097. (e) Cornelissen, J. J. L. M.; Rowan, A. E.; Nolte, R. J. M.; Sommerdijk, N. A. J. M. *Chem. Rev.* **2001**, *101*, 4039−4070. (f) Green, M. M.; Peterson, N. C.; Sato, T.; Teramoto, A.; Cook, R.; Lifson, S. *Science* **1995**, *268*, 1860−1866. (g) Fujiki, M. *Macromol. Rapid Commun.* **2001**, *22*, 539−563.

10.1021/ja035040s CCC: $25.00

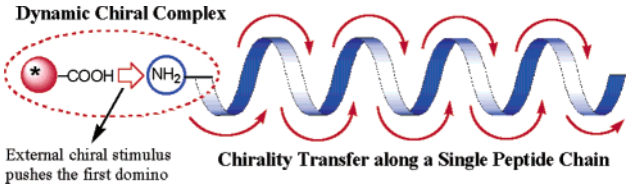

Figure 1. The NCDE principle leading to the induction of a one-handed helix for a single peptide chain (modified from refs 7,8).

another unique noncovalent chiral induction on one terminus of an optically inactive helical peptide.[7,8] Herein, a 3_{10}-helical backbone composed of unusual achiral α-amino acids, which alone adopts no preferred screw sense in solution, undergoes the excess of a one-handed helix through the addition of chiral small carboxylic acid. Our previous results[9] suggest that the external chiral stimulus operates on the N-terminal amino group to generate a chiral environment at the N-terminus, in turn leading to continuous chirality transfer to the C-terminus along the single achiral chain. We have defined this terminus-triggered chiral induction as the "noncovalent chiral domino effect (NCDE)",[7,8,10,11] as it is like a domino-toppling game along a single peptide chain (Figure 1).

As already found in artificial backbones[12] and oligopeptides,[13] a one-handed helicity of a single achiral chain is predominantly induced by a chiral moiety covalently incorporated into one terminus. Such terminal chiral induction, according to our definition,[8,11] might be termed as the "covalent chiral domino effect (CCDE)". The CCDE, in fixed conditions such as temperature and solvent, might provide an intrinsic screw-sense bias for achiral segment. In contrast, the noncovalent type will enable one to control the original helicity through external chiral stimulus. In fact, the helicity or helical stability of chiral peptides is markedly influenced by the NCDE.[10,11]

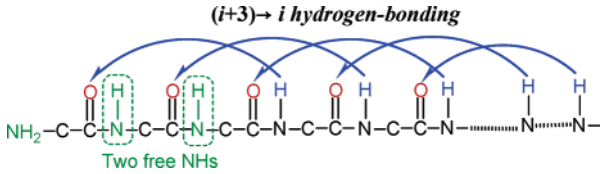

Figure 2. Intramolecular hydrogen-bonding scheme of a 3_{10}-helix.

Furthermore, the NCDE well-mimics biological systems in the following two points of view. First, the backbone exemplified for the NCDE is composed of achiral "α-amino acid" residues. This system thus has peculiar appeal for bearing close structural similarities to natural proteins and (poly)peptides that are made of "α-amino acid" residues. In other words, natural peptide helices might possess novel underlying properties leading to the NCDE. Second, the NCDE has been demonstrated on 3_{10}-helical peptides with a free N-terminus. A 3_{10}-helix[14] is characterized by a pitch of three residues per turn accompanied with consecutive 10-membered hydrogen bonds of a NH (i+3)→CO i pair, as illustrated in Figure 2. The helix is frequently found in native proteins and peptides as a subtype of the α-helix, playing a vital role for building up ternary protein structures. In particular, natural α-helical chains often adopt a 3_{10}-helix for the N- or C-terminal sequence.[14e,f,h] Consequently, the NCDE should provide novel insights into chiral recognition and amplification applicable to a great number of natural 3_{10}-helical segments.

Although the NCDE principle involves many new significant aspects in biological chiral interactions, the detailed mechanism

(2) (a) Yashima, E.; Matsushima, T.; Okamoto, Y. *J. Am. Chem. Soc.* **1997**, *119*, 6345−6359. (b) Ishikawa, M.; Maeda, K.; Yashima, E. *J. Am. Chem. Soc.* **2002**, *124*, 7448−7458. (c) Schlitzer, D. S.; Novak, B. M. *J. Am. Chem. Soc.* **1998**, *120*, 2196−2197. (d) Majidi, M. R.; Kane-Maguire, L. A. P.; Wallace, G. G. *Polymer* **1994**, *35*, 3113−3115. (e) Reece, D. A.; Kane-Maguire, L. A. P.; Wallace, G. G. *Synth. Met.* **2001**, *119*, 101−102. (f) Majidi, M. R.; Ashraf, S. A.; Kane-Maguire, L. A. P.; Norris, I. D.; Wallace, G. G. *Synth. Met.* **1997**, *84*, 115−116. (g) Yashima, E.; Maeda, K.; Yamanaka, T. *J. Am. Chem. Soc.* **2000**, *122*, 7813−7814. (h) Onouchi, H.; Maeda, K.; Yashima, E. *J. Am. Chem. Soc.* **2001**, *123*, 7441−7442. The induced helicity can be "memorized" upon the replacement of chiral interactive molecules by achiral ones. For the details, see: (i) Yashima, E.; Maeda, K.; Okamoto, Y. *Nature* **1999**, *399*, 449−451. Also, the original helicity of a chiral polymer was shown to be inverted through chiral stimuli of small molecules. See: (j) Yashima, E.; Maeda, Y.; Okamoto, Y. *J. Am. Chem. Soc.* **1998**, *120*, 8895−8896.

(3) An optically inactive polymer was shown to prefer a one-handed helix in chiral solvent. For elegant examples, see: (a) Green, M. M.; Khatri, C.; Peterson, N. C. *J. Am. Chem. Soc.* **1993**, *115*, 4941−4942. (b) Khatri, C. A.; Pavlova, Y.; Green, M. M.; Morawetz, H. *J. Am. Chem. Soc.* **1997**, *119*, 9, 6991−6995. (c) Dellaportas, P.; Jones, R. G.; Holder, S. J. *Macromol. Rapid Commun.* **2002**, *23*, 99−103.

(4) Moore and co-workers proposed a unique chiral induction that a cylindrical inner space created by helical formation of an achiral backbone captures a chiral molecule to induce a predominantly one-handed helix.[1c] See also: Prince, R. B.; Barnes, S. A.; Moore, J. S. *J. Am. Chem. Soc.* **2000**, *122*, 2758−2762.

(5) The irradiation of a one-handed circularly polarized light as external chiral source gives rise to the induction of helicity of a polymer. See: Li, J.; Schuster, G. B.; Cheon, K.-S.; Green, M. M.; Selinger, J. V. *J. Am. Chem. Soc.* **2000**, *122*, 2603−2612.

(6) As for noncovalent chiral induction of achiral peptide, Nielsen and coworkers have already proposed an elegant system that an achiral peptide nucleic acid (PNA) backbone undergoes chiral duplex formation with the complementary PNA chain containing a chiral residue at the N- or C-terminus, wherein the chiral induction occurs basically through the side-chain base pairings. For the details, see: (a) Wittung, P.; Nielsen, P. E.; Buchardt, O.; Egholm, M.; Nordén, B. *Nature* **1994**, *368*, 561−563. (b) Kozlov, I. A.; Orgel, L. E.; Nielsen, P. E. *Angew. Chem., Int. Ed.* **2000**, *39*, 4292−4295. (c) Wittung, P.; Eriksson, M.; Lyng, R.; Nielsen, P. E.; Nordén, B. *J. Am. Chem. Soc.* **1995**, *117*, 10167−10173. (d) Sforza, S.; Haaima, G.; Marchelli, R.; Nielsen, P. E. *Eur. J. Org. Chem.* **1999**, *1*, 197−204.

(7) Inai, Y.; Tagawa, K.; Takasu, A.; Hirabayashi, T.; Oshikawa, T.; Yamashita, M. *J. Am. Chem. Soc.* **2000**, *122*, 11731−11732.

(8) Inai, Y. *Recent Research Developments in Macromolecules*; Research Signpost: India, 2002; Chapter 2.

(9) The following facts imply that the interaction occurs at the N-terminus:[7,8] (i) the induced CD amplitude was substantially ascribed to the fraction of complexion; (ii) no chiral induction was observed for the N-protected achiral peptide, irrespective of the addition of a large excess of chiral acid.

(10) Inai, Y.; Ishida, Y.; Tagawa, K.; Takasu, A.; Hirabayashi, T. *J. Am. Chem. Soc.* **2002**, *124*, 2466−2473.

(11) Inai, Y.; Komori, H.; Takasu, A.; Hirabayashi, T. *Biomacromolecules* **2003**, *4*, 122−128.

(12) (a) Okamoto, Y.; Matsuda, M.; Nakano, T.; Yashima, E. *Polym. J.* **1993**, *25*, 391−396. (b) Maeda, K.; Okamoto, Y. *Polym. J.* **1998**, *30*, 100−105. (c) Obata, K.; Kabuto, C.; Kira, M. *J. Am. Chem. Soc.* **1997**, *119*, 11345−11346. (d) Obata, K.; Kira, M. *Macromolecules* **1998**, *31*, 4666−4668. (e) Mizutani, T.; Yagi, S.; Morinaga, T.; Nomura, T.; Takagishi, T.; Kitagawa, S.; Ogoshi, H. *J. Am. Chem. Soc.* **1999**, *121*, 754−759.

(13) (a) Pieroni, O.; Fissi, A.; Pratesi, C.; Temussi, P. A.; Ciardelli, F. *J. Am. Chem. Soc.* **1991**, *113*, 6338−6340. (b) Pengo, B.; Formaggio, F.; Crisma, M.; Toniolo, C.; Bonora, G. M.; Broxterman, Q. B.; Kamphuis, J.; Saviano, M.; Iacovino, R.; Rossi, F.; Benedetti, E. *J. Chem. Soc., Perkin Trans. 2* **1998**, 1651−1657. (c) Crisma, M.; Valle, G.; Formaggio, F.; Toniolo, C. *Z. Kristallogr.* **1998**, *213*, 599−604. (d) Benedetti, E.; Saviano, M.; Iacovino, R.; Pedone, C.; Santini, A.; Crisma, M.; Formaggio, F.; Toniolo, C.; Broxterman, Q. B.; Kamphuis, J. *Biopolymers* **1998**, *46*, 433−443. (e) Toniolo, C.; Saviano, M.; Iacovino, R.; Crisma, M.; Formaggio, F.; Benedetti, E. *Z. Kristallogr.* **1999**, *214*, 160−166. (f) Pieroni, O.; Fissi, A.; Pratesi, C.; Temussi, P. A.; Ciardelli, F. *Biopolymers* **1993**, *33*, 1−10. (g) Tuzi, A.; Ciajolo, M. R.; Picone, D.; Crescenzi, O.; Temussi, P. A.; Fissi, A.; Pieroni, O. *J. Pept. Sci.* **1996**, *2*, 47−58. (h) Bhargava, K.; Rao, R. B. *Lett. Pept. Sci.* **2002**, *8*, 41−45. (i) Inai, Y.; Kurokawa, Y.; Hirabayashi, T. *Biopolymers* **1999**, *49*, 551−564. (j) Inai, Y.; Ashitaka, S.; Hirabayashi, T. *Polym. J.* **1999**, *31*, 246−253.

(14) (a) Taylor, H. S. *Proc. Am. Philos. Soc.* **1941**, *85*, 1−7. (b) Huggins, M. L. *Chem. Rev.* **1943**, *32*, 195−218. (c) Bragg, W. L.; Kendrew, J. C.; Perutz, M. F. *Proc. R. Soc. London, Ser. A* **1950**, *203*, 321−357. (d) Donohue, J. *Proc. Natl. Acad. Sci. U.S.A.* **1953**, *39*, 470−478. (e) Barlow, D. J.; Thornton, J. M. *J. Mol. Biol.* **1988**, *201*, 601−619. (f) Toniolo, C.; Benedetti, E. *Trends Biochem. Sci.* **1991**, *16*, 350−353. (g) Topol, I. A.; Burt, S. K.; Deretey, E.; Tang, T.-H.; Perczel, A.; Rashin, A.; Csizmadia, I. G. *J. Am. Chem. Soc.* **2001**, *123*, 6054−6060. (h) Richardson, J. S.; Richardson, D. C. In *Prediction of Protein Structure and the Principles of Protein Conformation*; Fasman, G. D., Ed.; Plenum Press: New York, 1989; pp 1−98. (i) Smythe, M. L.; Huston, S. E.; Marshall, G. R. *J. Am. Chem. Soc.* **1995**, *117*, 5445−5452.

still remains open. In particular, little is known about the structural information of a dynamic complex of peptide with chiral additive. In addition, we have no answer as to why a complex generated around the N-terminus gives rise to a predominant induction of a one-handed helix.

We here propose a dynamic structure in the complexation of the N-terminal segment of a 3_{10}-helix with a chiral acid molecule in solution. Previously, the achiral helicogenic sequence, H-(Aib-Δ^ZPhe)$_4$- (Aib = α-aminoisobutyric acid; Δ^ZPhe = (*Z*)-α,*β*-didehydrophenylalanine), was employed as a common scaffold for the NCDE.[7,8,10,11] Here, a large excess of chiral acid (<ca. 600-fold) is required for sufficient chiral induction of the peptide because of the sterically hindered amino group of the N-terminal Aib residue. Such a higher concentration of chiral species precludes the establishment of an appropriate NMR condition to focus on the signals of a peptide molecule in complexation. Accordingly, we newly synthesized the following peptide **1** where the original N-terminal Aib residue is substituted by a more flexible *β*-alanine (*β*-Ala)[15] to enhance the binding affinity to chiral acid.

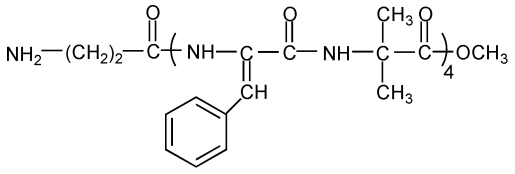

H-β-Ala-(Δ^ZPhe-Aib)$_4$-OMe (**1**) (OMe = methoxy).

NMR and CD spectroscopy was performed for a solution of peptide **1** with chiral acid to obtain experimental information about the dynamic complex. In parallel, molecular modeling based on energy computation proposes a rational structure of the peptide-chiral acid complex. Consequently, chiral acid enabling chiral induction needs to possess at least both one carboxyl and one urethane (or amide) groups as the so-called "peptide acid". In the complexation, the N-terminal 3_{10}-helical segment bearing two free amide NH's, H-*β*-Ala(1)-Δ^ZPhe(2)-NH-, captures effectively such a peptide acid molecule through three-point interactions to generate a chiral environment. To our best knowledge, this is the first proof of the existence of novel chiral interactions on a 3_{10}-helical terminus, "chiral recognition" and "chirality transfer". A 3_{10}-helix can recognize the chirality of external peptide acid on its N-terminal backbone, and subsequently the chiral signal acquired at the terminus runs along the following helical chain, finally leading to dynamic control of the original helicity and helical stability. Therefore, the present conclusion provides new paradigm for chiral biological interactions on the termini of an enormous number of naturally occurring helical segments.

Results and Discussion

Solution Conformation of Peptide 1. The segment -(Aib-Δ^ZPhe)$_3$- of peptide **1** can be expected to generate two enantiomeric (left-handed and right-handed) helices, because Aib or Δ^ZPhe residues show the strong tendency to form a 3_{10}-helix.[16] Also, oligopeptides bearing -(Aib-Δ^ZPhe)$_m$- ($m = 2-4$) are prone to adopt a typical 3_{10}-helical structure in solution and in the solid states.[7,8,10,11,13i,j,17] Helix formation of peptide **1** in solution was experimentally evidenced as follows. The NOESY spectrum in $CDCl_3$ gave marked cross-peaks of $N_iH-N_{i+1}H$ resonances in the segment from Aib(3) to Aib(9), thus indicating the presence of a 3_{10}-helix or an α-helix.[18] From the variation in NH chemical shifts of peptide **1** with concentration of $(CD_3)_2SO$[19] in $CDCl_3$ (Figure 3), six NH resonances of Δ^ZPhe(4) to Aib(9) residues were shown to be shielded from solvent due to intramolecular hydrogen bonding, of which the pattern corre-

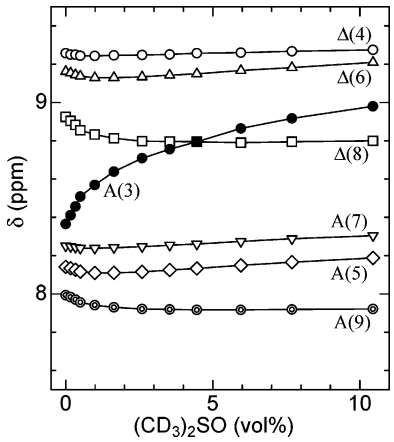

Figure 3. Solvent dependence on NH chemical shifts of peptide **1** in $CDCl_3$/$(CD_3)_2SO$ mixtures at 293 K in 200 MHz ^{1}H NMR spectra. The Δ^ZPhe(2) NH resonance could not be observed due to its broadening throughout the titration.

(15) Cheng, R. P.; Gellman, S. H.; DeGrado, W. F. *Chem. Rev.* **2001**, *101*, 3219−3232.

(16) For 3_{10}-helices of Aib-based[a−j] and Δ^ZPhe-based[k−u] oligopeptides, see: (a) Benedetti, E.; Bavoso, A.; Di Blasio, B.; Pavone, V.; Pedone, C.; Crisma, M.; Bonora, G. M.; Toniolo, C. *J. Am. Chem. Soc.* **1982**, *104*, 2437−2444. (b) Prasad, B. V. V.; Balaram, P. *CRC Crit. Rev. Biochem.* **1984**, *16*, 307−348. (c) Karle, I. L.; Flippen-Anderson, J. L.; Uma, K.; Balaram, H.; Balaram, P. *Proc. Natl. Acad. Sci. U.S.A.* **1989**, *86*, 765−769. (d) Toniolo, C.; Bonora, G. M.; Bavoso, A.; Benedetti, E.; Di Blasio, B.; Pavone, V.; Pedone, C. *Macromolecules* **1986**, *19*, 472−479. (e) Toniolo, C.; Crisma, M.; Bonora, G. M.; Benedetti, E.; Di Blasio, B.; Pavone, V.; Pedone, C.; Santini, A. *Biopolymers* **1991**, *31*, 129−138. (f) Toniolo, C.; Benedetti, E. *Macromolecules* **1991**, *24*, 4004−4009 and references therein. (g) Benedetti, E.; Di Blasio, B.; Pavone, V.; Pedone, C.; Toniolo, C.; Crisma, M. *Biopolymers* **1992**, *32*, 453−456. (h) Otoda, K.; Kitagawa, Y.; Kimura, S.; Imanishi, Y. *Biopolymers* **1993**, *33*, 1337−1345. (i) Okuyama, K.; Ohuchi, S. *Biopolymers* **1996**, *40*, 85−103. (j) Venkatraman, J.; Shankaramma, S. C.; Balaram, P. *Chem. Rev.* **2001**, *101*, 3131−3152. (k) Ciajolo, M. R.; Tuzi, A.; Pratesi, C. R.; Fissi, A.; Pieroni, O. *Biopolymers* **1990**, *30*, 911−920. (l) Ciajolo, M. R.; Tuzi, A.; Pratesi, C. R.; Fissi, A.; Pieroni, O. *Int. J. Pept. Protein Res.* **1991**, *38*, 539−544. (m) Ciajolo, M. R.; Tuzi, A.; Pratesi, C. R.; Fissi, A.; Pieroni, O. *Biopolymers* **1992**, *32*, 717−724. (n) Bhandary, K. K.; Chauhan, V. S. *Biopolymers* **1993**, *33*, 209−217. (o) Rajashankar, K. R.; Ramakumar, S.; Chauhan, V. S. *J. Am. Chem. Soc.* **1992**, *114*, 9225−9226. (p) Padmanabhan, B.; Singh, T. P. *Biopolymers* **1993**, *33*, 613−619. (q) Jain, R.; Chauhan, V. S. *Biopolymers* **1996**, *40*, 105−119. (r) Jain, R. M.; Rajashankar, K. R.; Ramakumar, S.; Chauhan, V. S. *J. Am. Chem. Soc.* **1997**, *119*, 3205−3211. (s) Mitra, S. N.; Dey, S.; Karthikeyan, S.; Singh, T. P. *Biopolymers* **1997**, *41*, 97−105. (t) Ramagopal, U. A.; Ramakumar, S.; Sahal, D.; Chauhan, V. S. *Proc. Natl. Acad. Sci. U.S.A.* **2001**, *98*, 870−874. (u) Ramagopal, U. A.; Ramakumar, S.; Mathur, P.; Joshi, R.; Chauhan, V. S. *Protein Eng.* **2002**, *15*, 331−335.

(17) (a) Inai, Y.; Kurokawa, Y.; Kojima, N. *J. Chem. Soc., Perkin. Trans. 2* **2002**, 1850−1857. (b) Inai, Y.; Kurokawa, Y.; Hirabayashi, T. *Macromolecules* **1999**, *32*, 4575−4581. (c) Inai, Y.; Oshikawa, T.; Yamashita, M.; Hirabayashi, T.; Ashitaka, S. *J. Chem. Soc., Perkin. Trans. 2* **2001**, 892−897.

(18) The NOESY spectrum of peptide **1** alone did not show marked cross-peaks for backbone proton pairs other than NH_i-NH_{i+1}. However, this NOE pattern should reflect energy-minimized peptide **1**, where a distance of NH_i-NH_{i+1} ranges from 3.0 to 3.5 Å, while that of NH_i-NH_{i+2} is considerably large (4.8−5.0 Å). When peptide **1** adopts a standard α-helix, a similar NOE pattern should be expected: that is, shorter NH_i-NH_{i+1} (2.8−2.9 Å) and longer NH_i-NH_{i+2} (4.3−4.4 Å). Accordingly, we can hardly distinguish between both helices using only the NOESY data lacking $C^\alpha H$ proton. For the relationship between the NOE pattern and expected secondary structure of proteins, see: Wüthrich, K.; Billeter, M.; Braun, W. *J. Mol. Biol.* **1984**, *180*, 715−740.

(19) For the method to identify peptide NH's exposed to solvent, see: Pitner, T. P.; Urry, D. W. *J. Am. Chem. Soc.* **1972**, *94*, 1399−1400.

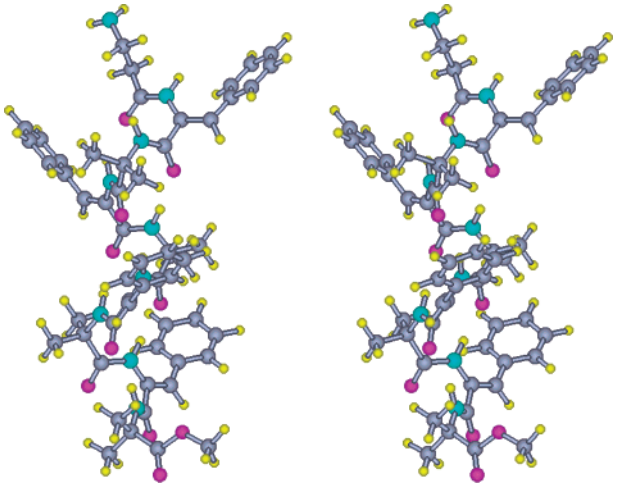

Figure 4. A stereoview of peptide **1** energy-minimized by the semiempirical MO calculation (AM1 method).[21] The converged structure from a standard 3_{10}-helix retained a typical 3_{10}-helical conformation (the right-handed helix is shown here).

sponds to a 3_{10}-helix[14,16] supported by consecutive $(i+3) \rightarrow i$ hydrogen bonds starting from NH Δ^ZPhe(4) → CO Aib(1), as shown in Figure 2.

The temperature dependence on 600 MHz ^{1}H NMR spectra of peptide **1** in $CDCl_3$ was also investigated at 293−268 K. As the most striking feature, a broad band of Δ^ZPhe(2) NH newly appeared far downfield (9.5 ppm) below 283 K. The temperature coefficients ($-\Delta\delta/\Delta T$ in ppb/deg) for all of the amide protons were obtained with a good linearity as follows: 9.0 [Δ^ZPhe(2)], 17.7 [Aib(3)], 5.2 [Δ^ZPhe(4)], 2.9 [Aib(5)], 4.5 [Δ^ZPhe(6)], 1.7 [Aib(7)], 4.4 [Δ^ZPhe(8)], and 2.9 [Aib(9)]. Obviously, the two NH resonances of Δ^ZPhe(2) and Aib(3) residues giving a considerably large value are indicative of exposure to solvent, while the remaining NH's are shielded due to the intramolecular hydrogen bonding, of which the pattern confirms the evidence for a 3_{10}-helix.

The helical conformation was also supported by the FT-IR spectrum in chloroform; that is, the positions of amide I absorption bands were 1658 and 1625 cm^{-1}, which can be assigned to saturated amino acid and Δ^ZPhe residues in helical segments,[20] respectively. Furthermore, energy minimization of peptide **1** by the semiempirical molecular orbital (MO) calculation (AM1 method in MOPAC97)[21] afforded a typical 3_{10}-helical conformation as shown in Figure 4; the average values for Δ^ZPhe(2)−Δ^ZPhe(8) residues were $\langle\phi\rangle = -39.4°$, $\langle\psi\rangle = -40.4°$, and $\langle\omega\rangle = 179.4°$. In Figure 4, six NH's of Δ^ZPhe(4)−Aib(9) residues, as experimentally found, participated in consecutive $(i+3)$th NH → ith CO hydrogen bonds, appropriate for a 3_{10}-helix. Therefore, peptide **1** alone was shown experimentally and theoretically to adopt a typical 3_{10}-helical conformation in solution.

Chiral Induction through Boc-Amino Acid. Achiral peptide **1** alone displayed no CD signals in solution, wherein the chiral symmetry is being strictly conserved to yield both left-handed and right-handed helices in an equimolar amount (Figure 5, dotted line). However, when to a chloroform solution of peptide **1** was added enantiomerically pure Boc-L-Pro-OH (Boc = *tert*-butoxycarbonyl), intense split CD signals were induced around 283 nm assignable to Δ^ZPhe residues (Figure 5). The mirror image was obtained by the addition of Boc-D-Pro-OH, thus indicating that the induced CD signals are responsible for the chiral interaction of peptide **1** with Boc-Pro-OH, but not relevant to some accidental impurities or spectroscopic artifacts.

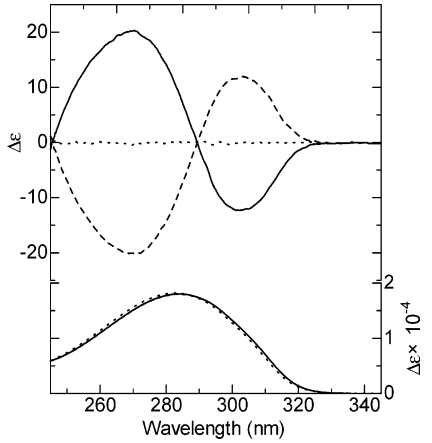

Figure 5. CD (top) and UV absorption (bottom) spectra of peptide **1** (dotted line) in chloroform and of that in the presence of Boc-L-Pro-OH (solid line) and Boc-D-Pro-OH (broken line): [**1**] = 0.14 mM and [Boc-Pro-OH] = 5 mM. $\Delta\epsilon$ and ϵ are expressed with respect to the molar concentration of Δ^ZPhe residues. The far-UV CD region is impossible to analyze for the following reasons: (i) chloroform is not transparent below 230−240 nm; (ii) a large excess of Boc-amino acid hides the peptide-bond absorption; (iii) in general, Δ^ZPhe residue offers an absorption band around 220 nm, which couples with amide transition to preclude conventional far-UV CD analysis.[8,22b]

Table 1. Signs of Splitting Cotton Effects and $\Delta\epsilon$ Values for Induced CD of Peptide **1** with Chiral Boc-Amino Acid[a]

	first Cotton effect		second Cotton effect	
Boc-amino acid	sign	$\Delta\epsilon/\lambda$ (nm)	sign	$\Delta\epsilon/\lambda$ (nm)
Boc-L-Pro-OH	−	12.3/302	+	20.3/270
Boc-D-Pro-OH	+	12.0/302	−	20.2/270
Boc-L-Ala-OH	−	9.9/302	+	16.0/269
Boc-L-Val-OH	−	11.6/303	+	18.5/269
Boc-L-Leu-OH	−	12.6/302	+	20.5/269
Boc-L-Phe-OH	−	8.4/302	+	12.7/269

[a] [**1**] = 0.14 mM and [Boc-amino acid] = 5 mM in chloroform.

The split CD pattern with a negative peak at longer wavelengths and a positive peak at shorter wavelengths (− to +) was similarly observed for the other Boc-L-amino acids, as shown in Table 1. The absorption band around 280 nm has been assigned to charge transfer between the styryl and carbonyl groups in the Δ^ZPhe residue.[22] (For a detailed CD analysis of Δ^ZPhe-containing peptides, see ref 22b.) In addition, the corresponding transition moments were theoretically estimated to lie approximately on a $C^\gamma-C^\alpha$ line (roughly speaking, side chain to helix backbone).[23,24] Thus, the CD sign of (− to +), on the basis of the exciton chirality method,[25] can be assigned to a counterclockwise twist for the neighboring pair of the transition moments, thereby corresponding to a right-handed

(20) (a) Inai, Y.; Sakakura, Y.; Hirabayashi, T. *Polym. J.* **1998**, *30*, 828−832. (b) Kennedy, D. F.; Crisma, M.; Toniolo, C.; Chapman, D. *Biochemistry* **1991**, *30*, 6541−6548. A shift to lower wavenumbers in the second peak should be ascribed to partial contribution of resonance between carbonyl and styryl groups in a Δ^ZPhe residue.[10,20a]

(21) The AM1 method in MOPAC97 was employed: Dewar, M. J. S.; Zoebisch, E. G.; Healy, E. F.; Stewart, J. J. P. *J. Am. Chem. Soc.* **1985**, *107*, 3902−3909. For MOPAC97, see: Stewart, J. J. P. MOPAC97; Fujitsu Ltd., Tokyo, Japan, 1998.

(22) (a) Pieroni, O.; Montagnoli, G.; Fissi, A.; Merlino, S.; Ciardelli, F. *J. Am. Chem. Soc.* **1975**, *97*, 6820−6826. (b) Pieroni, O.; Fissi, A.; Jain, R. M.; Chauhan, V. S. *Biopolymers* **1996**, *38*, 97−108.

screw sense for the 3_{10}-helix or α-helix. Consequently, the addition of Boc-L-amino acid induces a predominantly right-handed helix for the achiral peptide. The direction of the helical screw sense induced by Boc-L-amino acid agreed with those observed for H-(Aib-Δ^ZPhe)$_4$-Aib-OMe (**2**)[7] and H-(Aib-Δ^ZPhe)$_4$-L-Leu-OMe.[10]

For the elucidation of stoichiometry in chiral induction, a Job plot of induced CD amplitude versus peptide/Boc-L-Leu-OH molar ratio was performed.[26] It exhibited a convex profile having a maximum CD signal at equimolar concentration, thus proving that chiral indication is based on the 1:1 binding of a peptide molecule to a Boc-amino acid molecule. The equimolar stoichiometry is also supported by a good linearity between induced CD amplitude and enantiomer excess of Boc-amino acid.[27] In other words, there is no positive nonlinear effect found in chiral induction based on two or more chiral molecules that operate covalently[1f,g,28] or noncovalently[2a,29] on a single helical chain. Thus, a single Boc-amino acid molecule induces the helicity of a single peptide molecule.

Figure 6 shows the relationship between the chiral additive concentration and the induced CD amplitude. The CD signal increases drastically with an increase in the Boc-L-Pro-OH or Boc-L-Leu-OH concentration ranging from 0 to 2.5 (17-fold) mM, and it reaches substantially a saturation value over 6 mM.

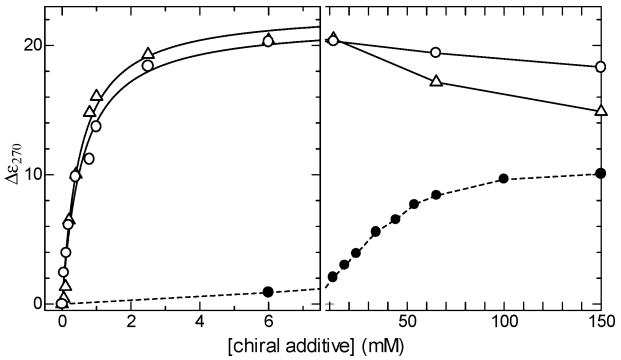

Figure 6. Titration curve of induced CD amplitude at 270 nm ($\Delta\epsilon_{270}$) in the complexation of peptide **1** (0.15 mM) with concentration of Boc-L-Pro-OH (○) or Boc-L-Leu-OH (△) in chloroform at 293 K. For comparison, the titration of peptide **2**-Boc-L-Pro-OH (●) was superimposed.[7] The left panel displays the titration profiles for chiral additive concentrations ranging from 0 to 7 mM, and further titration data (10−150 mM) are shown in the right panel. In the left panel, the two solid curves for peptide **1** are drawn from the nonlinear fitting of the corresponding CD data (0−6 mM) for the estimation of K_{app}.

Meanwhile, the saturated value is somewhat decreased by the addition of a large excess of Boc-L-amino acid. This behavior is most likely to occur due to the complexation of a 1:2 peptide-chiral guest enfeebling a chiral bias generated by a 1:1 complex. Similar behavior was observed for the addition of a large excess of chiral diamine to a 1:1 complex of zinc porphyrin tweezer-diamine.[30]

The titration curve for achiral peptide **2** with Boc-L-Pro-OH[7] is superimposed therein. Two striking features can be drawn through a brief comparison between both peptides. First, chiral induction of peptide **1** is attained by a much smaller amount of chiral additive, as compared to that of peptide **2**. From nonlinear fitting of the initial titration data (0−6 mM), the apparent binding constant (K_{app}, M^{-1}) was estimated to be 1.9×10^3 for **1**-Boc-L-Pro-OH, and 2.2×10^3 for **1**-Boc-L-Leu-OH, while it was 28 for **2**-Boc-L-Pro-OH.[7] The high binding affinity of peptide **1** to Boc-L-amino acid, as expected in the Introduction section, should result from N-terminal substitution of Aib residue having a sterically hindered amino group by more flexible β-Ala. Second, the maximum CD value observed for peptide **1** was about twice as large as that for peptide **2**. This reveals that a stronger screw-sense bias can be generated by a dynamic complex of peptide **1**, where the more flexible N-terminal segment will be advantageous for generating an effective chiral bias.

Structural Requirement of Additive for Chiral Induction. In the preceding section and our previous CD studies,[7,8,10,11]

(23) We have treated Δ^ZPhe residue as a planar trans cinnamic group according to ref 22a. The theoretical calculation (PPP-MO)[24a−d] on the cinnamic group demonstrated that the transition moment around 280 nm is located on the C′−C$^\alpha$−C$^\beta$−C$^\gamma$ plane, being directed from the midpoint of C$^\beta$−C$^\gamma$ to a position on C$^\alpha$−C′.[24e,f] The theoretical CD calculation using this dipole moment indicated that a segment -(Aib-Δ^ZPhe)$_m$- in a right-handed 3_{10}- or α-helix generates split CD signals of (− to +).[7,10,13i,24e,f] On the other hand, all of the four Δ^ZPhe residues in energy-minimized peptide **1** (Figure 4) are indeed in a nonplanar conformation (ϕ, ψ, $\chi^2 \neq 0$ or 180°). For more precise estimation of the excited state, an INDO/S[24g−i] calculation was carried out for nonplanar CH_3-CO-Δ^ZPhe-NH-CH_3, of which the atomic coordinates were extracted from each of four units C$^\alpha$-CO-Δ^ZPhe-NH-C$^\alpha$ in a right-handed 3_{10}-helical peptide **1** induced by the binding of Boc-L-Leu-OH, which will be shown later in Figure 15A. The combination of 14 higher occupied MOs and 14 lower occupied MOs ($14^2 = 196$ states) was used for the singly excited configuration interaction (SCI). As a result, the largest oscillator strength ($f = 0.65-0.70$) for each Δ^ZPhe residue was found at 272−278 nm, being consistent with the experimental absorption profile. The corresponding transition moments were shown to lie approximately on a C$^\gamma$−C$^\alpha$ line (roughly speaking, side chain to helix backbone). For the graphical location of each transition moment in the right-handed 3_{10}-helix, see the Supporting Information. In the top view of the helix from the N-terminus, the transition moments are spatially arranged with a counterclockwise fashion for the neighboring pairs. The exciton chirality method[25] for the system clarifies that the right-handed 3_{10}-helix affords a split CD sign with a negative peak at longer wavelengths. Therefore, the INDO/S-SCI result does not alter the previous CD assignment. Also, the experimental CD assignment was proven by the relationship between the split CD sign and X-ray structure. Analogous peptide Boc-L-Pro-(Aib-Δ^ZPhe)$_2$-Aib-OMe was found in a left-handed 3_{10}-helix in the crystal state.[17c] The hexapeptide, which retained a 3_{10}-helix in solution, showed reasonably exciton splitting of (+ to −) centered at 280 nm.[8,24j]

(24) (a) Pariser, R.; Parr, R. G. *J. Chem. Phys.* **1953**, *21*, 466−471. (b) Pariser, R.; Parr, R. G. *J. Chem. Phys.* **1953**, *21*, 767−776. (c) Pople, J. A. *Trans. Faraday Soc.* **1953**, *49*, 1375−1385. (d) Tokita, S.; Matsuoka, M.; Kogo, Y.; Kihara, H. *Molecular Design of Functional Coloring Matter: PPP Molecular Orbital Method and Its Application. (Kinosei Shikiso no Bunshi Sekkei: PPP Bunshi Kidoho to sono Katsuyo)*; Maruzen Co., Ltd.: Tokyo, Japan, 1989. (e) Inai, Y.; Ito, T.; Hirabayashi, T.; Yokota, K. *Biopolymers* **1993**, *33*, 1173−1184. (f) Inai, Y.; Ito, T.; Hirabayashi, T.; Yokota, K. *Polym. J.* **1995**, *27*, 846−855. (g) Ridley J.; Zerner, M. *Theor. Chim. Acta* **1973**, *32*, 111−134. (h) Zerner, M. C.; Loew, G. H.; Kirchner, R. F.; Mueller-Westerhoff, U. T. *J. Am. Chem. Soc.* **1980**, *102*, 589−599. (i) Matsuura, A. MOS-F 4.1; Fujitsu Ltd., Tokyo, Japan, 1998. (j) Inai, Y.; Kurokawa, Y.; Hirabayashi, T. *Bull. Chem. Soc. Jpn.* **1999**, *72*, 55−61.

(25) (a) Harada, N.; Chen, S. L.; Nakanishi, K. *J. Am. Chem. Soc.* **1975**, *97*, 5345−5352. (b) Harada, N.; Nakanishi, K. *Circular Dichroic Spectroscopy. Exciton Coupling in Organic Stereochemistry*; University Science Books: Mill Valley, CA, 1983.

(26) The figure is given in the Supporting Information. For the Job plot, see: Job, P. *Ann. Chim. Ser.* **1928**, *9*, 113−203.

(27) A linear relation was obtained between enantimoer excess (ee% = 0−100) of Boc-Thr-OH and the induced CD amplitude in chloroform; [Boc-Thr-OH] = 100 mM; [**1**] = 0.14 mM. ee is defined as ([L] − [D])/([L] + [D]).

(28) Such a covalent system was termed by Green and co-workers as "Majority Rules", stating that a small enantiomer excess in monomer compositions enables a one-handed helix for the resulting polymer. See: (a) Green, M. M.; Garetz, B. A.; Munoz, B.; Chang, H. P.; Hoke, S.; Cooks, R. G. *J. Am. Chem. Soc.* **1995**, *117*, 4181−4182. For other elegant examples, see: (b) Carlini, C.; Ciardelli, F.; Pino, P. *Makromol. Chem.* **1968**, *119*, 244−248. (c) Okamoto, Y.; Nishikawa, M.; Nakano, T.; Yashima, E.; Hatada, K. *Macromolecules* **1995**, *28*, 5153−5138. (d) Green, M. M.; Park, J.-W.; Sato, T.; Teramoto, A.; Lifson, S.; Selinger, R. L. B.; Selinger, J. V. *Angew. Chem., Int. Ed.* **1999**, *38*, 3138−3154. (e) Nomura, R.; Fukushima, Y.; Nakako, H.; Masuda, T. *J. Am. Chem. Soc.* **2000**, *122*, 8830−8836. (f) Takei, F.; Onitsuka, K.; Takahashi, S. *Polym. J.* **1999**, *31*, 1029−1032. (g) Benedetti, E.; De Simone, G.; Di Blasio, B.; Saviano, M.; Formaggio, F.; Polese, A.; Crisma, M.; Toniolo, C.; Kamphuis, J.; Aubry, A. *Gazz. Chim. Ital.* **1996**, *126*, 577−585.

(29) (a) Langeveld-Voss, B. M. W.; Waterval, R. J. M.; Janssen, R. A. J.; Meijer, E. W. *Macromolecules* **1999**, *32*, 227−230. (b) Nonokawa, R.; Yashima, E. *J. Am. Chem. Soc.* **2003**, *125*, 1278−1283.

(30) Kurtán, T.; Nesnas, N.; Li, Y.-Q.; Huang, X.; Nakanishi, K.; Berova, N. *J. Am. Chem. Soc.* **2001**, *123*, 5962−5973.

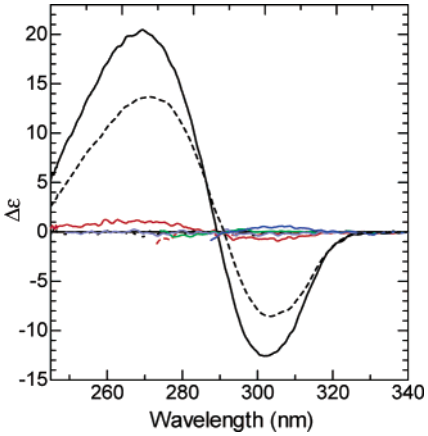

Figure 7. Induced CD spectra of peptide **1** (0.14 mM) in chloroform through addition of Boc-L-Leu-OH (5 mM: solid black), (*S*)-**3** (150 mM; solid green), (*S*)-**4** (150 mM; solid purple), (*S*)-**5** (65 mM; solid blue), (*R*)-**6** (150 mM; broken red), (*S*)-**7** (6 mM; broken black), or (*S*)-**8** (150 mM; solid red).

the NCDE was exemplified only for a limited chiral species, that is, Boc-amino acid. To clarify the chemical structure of the chiral molecule required for the NCDE, we here employed several dissimilar chiral additives for CD analysis. As shown in Figure 7, chiral carboxylic acids **3**−**5** gave only marginally small CD signals or no CD signals, irrespective of a large excess of their additives (65−150 mM).

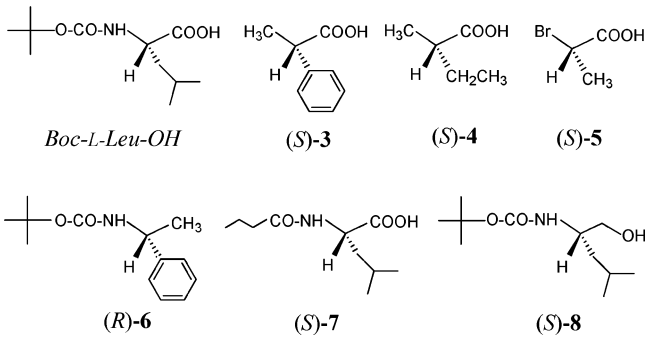

Likewise, no induced CD signals were observed for the addition of a large excess of chiral urethane **6**. These findings strongly suggest that a chiral molecule for generating chiral induction needs to possess at least both carboxyl and urethane groups. It is likely that the N-terminal segment of the achiral peptide simultaneously recognizes at least two chemical groups (carboxyl and urethane) of external chirality. Furthermore, chiral amide acid (*S*)-**7**, butyryl-L-Leu-OH, induces marked split CD signals similar to those of Boc-L-Leu-OH. This strongly supports the view that peptide **1** can interact simultaneously with carboxyl and amide groups of a so-called "peptide acid" to generate a chiral environment. Meanwhile, a marginally small CD signal was induced by Boc-L-leucinol (*S*)-**8**, of which a hydroxyl group as well as a urethane group might operate slightly on the N-terminal segment.

Through such multipoint interactions with a Boc-amino acid (or peptide acid) molecule, a dynamic chiral complex should be formed at the N-terminus to subsequently induce a predominantly one-handed helix for the following achiral segment. This speculation might agree with a general guideline for chiral recognition, that is, a "three-point rule"[31] stating that three simultaneous interactions are required at least for chiral

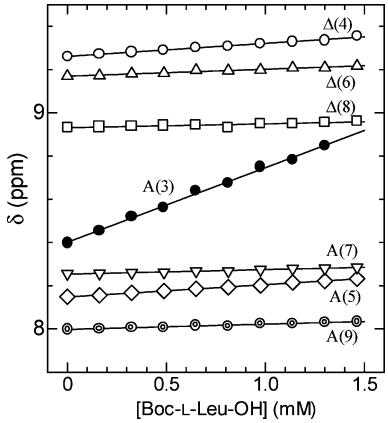

Figure 8. Dependence of Boc-L-Leu-OH concentration on NH chemical shifts of peptide **1** in $CDCl_3$ at 293 K in 200 MHz ^1H NMR spectra; [**1**] = 3.8 mM. Aib(3) NH disappeared above ca. 1.4 mM of Boc-L-Leu-OH.

discrimination of enantiomeric molecules. As far as oligopeptides are concerned, cyclic hexapeptide was shown to undergo chiral discrimination for Boc- or Fmoc-amino acid through three-point hydrogen-bonding complexation.[32]

NMR Studies of Dynamic Complexation. The acid−base interaction manner in aprotic organic solvents has been deeply discussed.[2a] Herein, in less apolar media such as chloroform, ion association should be predominant rather than the hydrogen-bonded ion pair.[2a,33] Thus, in chloroform of our present case, the amino group of peptide **1** and carboxyl group of Boc-amino acid will yield a contact-ion pair ($-COO^-\cdot NH_3^+-$) as its major species.[34]

The preceding CD results suggest that the N-terminal segment of a 3_{10}-helix involves a chiral recognition site. For more detailed structural information about a dynamic complex, NMR spectroscopy was performed for a mixture of peptide **1** and chiral additive. Figure 8 shows the variation of NH chemical shifts in $CDCl_3$ with the concentration of Boc-L-Leu-OH being a strong chiral inducer.

Six NH resonances of Δ^ZPhe(4) to Aib(9) residues are insensitive to an increasing concentration of the chiral additive, whereas the Aib(3) NH resonance is markedly shifted to a lower magnetic filed. Prior to the addition of Boc-amino acid, peptide **1** is folded into a 3_{10}-helix characterized by a (i+3) → i hydrogen-bond pattern shown in Figure 2; that is, the N-terminal two amide NH's of Δ^ZPhe(2) and Aib(3) residues are present as "free NH", whereas the other amide NH's participate in (i+3) → i hydrogen bonding. The addition of Boc-L-Pro-OH showed almost the same tendency in the NH resonance variations. Obviously, a Boc-amino acid molecule does bind to a free NH of the Aib(3) residue. Presumably, the chiral acid molecule should be captured by the N-terminal segment of H-β-Ala-Δ^ZPhe-Aib- through its two free amide NH's and amino terminus.

(31) (a) Dalgliesh, C. E. *J. Chem. Soc.* **1952**, 3940−3942. (b) Easson, L. H.; Stedman, E. *Biochem. J.* **1933**, *27*, 1257−1266. (c) Pirkle, W. H.; House, D. W. *J. Org. Chem.* **1979**, *44*, 1957−1960. (d) Pirkle, W. H.; Pochapsky T. C. *Chem. Rev.* **1989**, *89*, 347−362.
(32) McEwen, I. *Biopolymers* **1993**, *33*, 933−942.
(33) (a) Manabe, K.; Okamura, K.; Date, T.; Koga, K. *J. Am. Chem. Soc.* **1992**, *114*, 6940−6941. (b) Manabe, K.; Okamura, K.; Date, T.; Koga, K. *J. Am. Chem. Soc.* **1993**, *115*, 5324−5325.
(34) As an evidence for the major complexation manner, a chloroform solution of acetic acid with 1-propylamine, in fact, was shown to exhibit two strong vibrational bands characteristic of a carboxylate salt (1573 and 1404 cm^{-1}), while the original C=O stretching band completely disappeared.

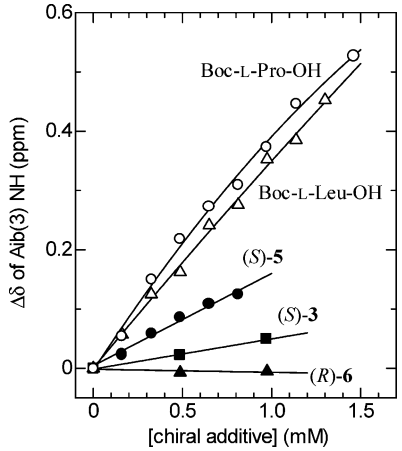

Figure 9. Dependence of chiral additive concentration on Aib(3) NH chemical shift of peptide **1** in $CDCl_3$ at 293 K in 200 MHz ^{1}H NMR spectra: Boc-L-Leu-OH, (*S*)-**3**, (*S*)-**5**, and (*R*)-**6** for [**1**] = 3.8 mM; Boc-L-Pro-OH for [**1**] = 3.4 mM.

The shift of the Aib(3) NH resonance should be an indicator to estimate the degree of interaction of the N-terminal segment with a chiral molecule. Addition of chiral carboxylic acid (*S*)-**3** or (*S*)-**5** showed a tendency similar to that of Boc-L-amino acid in NH variations; that is, the Aib(3) NH resonance was shifted to a lower magnetic filed, whereas six NH resonances of Δ^ZPhe(4) to Aib(9) residues were essentially retained. In contrast, the addition of chiral urethane (*R*)-**6** did not affect seven NH resonances of Aib(3)−Aib(9), which might reflect the fact that a compound having only a urethane carbonyl group leads to no chiral induction. These results strongly support that a carboxyl group forms a hydrogen bond with the free Aib(3) NH group. Figure 9 summarizes the plots of the shifting value of the Aib(3) NH resonance against the concentration of chiral species.

Interestingly, the Aib(3) NH binds to Boc-L-Leu-OH or Boc-L-Pro-OH more effectively than does normal chiral acid. Such a more favorable binding to Boc-amino acid should not originate from a difference in the acidity of carboxyl group, because (*S*)-**5** having a stronger acidity shows less effective binding than Boc-L-amino acid. Rather, the higher affinity for Boc-L-amino acid should be ascribed to the cooperative role of its urethane carbonyl group, which might interact with the other "free NH" of Δ^ZPhe(2) to facilitate the acid−base complexation.

The formation of a hydrogen bond between the Δ^ZPhe(2) NH and the urethane C═O of Boc-L-amino acid is evidenced by a similar titration experiment in 600 MHz ^{1}H NMR (Figure 10).

The addition of Boc-L-Pro-OH at 293 K induced a broad peak assignable to the Δ^ZPhe(2) NH resonance at lower magnetic fields (9.9−10 ppm). The emergence implies that the Δ^ZPhe-(2) NH resonance is being shielded from solvent due to the intermolecular hydrogen bond with Boc-L-amino acid. Interestingly, the addition of chiral carboxylic acid **3**, **5**, or chiral urethane **6** at a similar condition did not induce the Δ^ZPhe(2) NH resonance. From the NMR titration in Figure 9, chiral carboxylic acid **3** or **5** might be shown to undergo two-point interactions with the Aib(3) NH and N-terminal amino group of peptide **1**. Nevertheless, it does not induce a predominantly one-handed helix, according to the CD results (Figure 7). Furthermore, chiral urethane **6** does not form a hydrogen bond with either the Δ^ZPhe(2) NH or the Aib(3) NH group effectively.

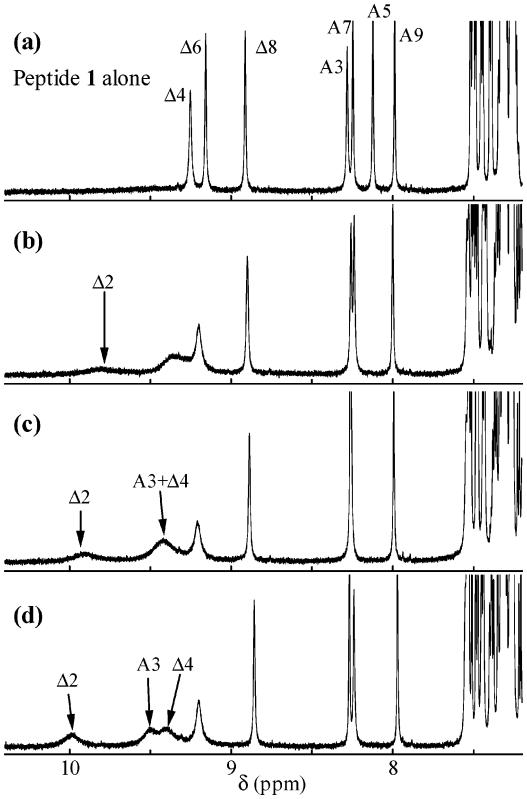

Figure 10. Expanded 600 MHz ^{1}H NMR spectra (NH and aromatic regions) of peptide **1** with Boc-L-Pro-OH in $CDCl_3$ at 293 K; [**1**] = 2.0 mM; [Boc-L-Pro-OH] = (a) 0, (b) 1.8, (c) 2.8, and (d) 4.6 mM. Δ and A denote Δ^ZPhe and Aib, respectively, and the number after Δ or A is the residue number from the N-terminus.

Thus, the additional hydrogen bond to Δ^ZPhe(2) NH can be dynamically formed by such a compound as Boc-amino acid, including at least both carboxyl and urethane carbonyl groups. From nonlinear fitting of the plot data of the Δ^ZPhe(2) NH resonance against Boc-L-Pro-OH concentration at 293 K, the K_{app} value was estimated to be 2.0×10^3 (M^{-1}),[35] being fully consistent with 1.9×10^3 obtained from the corresponding CD titration. Therefore, the formation of a hydrogen bond to Δ^ZPhe(2) NH is a significant process for achiral peptide **1** to recognize the chirality of a guest molecule to generate the NCDE.

In contrast, Boc-amino acid does not interact substantially with the segment -(Δ^ZPhe-Aib)$_3$-OMe, because these amide NH resonances are shielded due to the $(i+3) \rightarrow i$ intramolecular hydrogen bonds. As a result, the original 3_{10}-helix is essentially maintained in the chiral induction process. In other words, a Boc-amino acid molecule for the chiral induction operates only on the N-terminal segment. This fact provides important evidence for the NCDE.

At this stage, we can tentatively draw a dynamic complexation of the N-terminal segment with a Boc-amino acid molecule, as shown in Figure 11. First, the H-β-Ala's amino group binds to the carboxyl group to form a salt bridge, while either oxygen of the resulting carboxylate group is hydrogen-bonded to the

(35) The titration curve was obtained from the same experiment as Figure 10 ([**1**] = 2.0 mM at 293 K); Δ^ZPhe(2) NH resonance (ppm)−[Boc-L-Pro-OH] (mM) was 9.42−0, 9.56−0.6, 9.70−1.4, 9.80−1.8, 9.90−2.8, 9.95−3.6, 9.986−4.6, and 10.02−10.6. The Δ^ZPhe(2) NH resonance at [Boc-L-Pro-OH] = 0 mM, which did not appear at 293 K, was estimated from extrapolation to 293 K in a lower temperature dependence on the Δ^ZPhe(2) NH resonance.

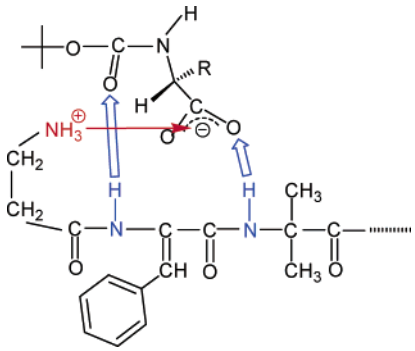

Figure 11. A proposed complexation between the N-terminal segment and Boc-amino acid for the NCDE.

free Aib(3) NH. Subsequently, the urethane carbonyl group forms a hydrogen bond to the free Δ^ZPhe(2) NH. Consequently, a looping complex is created through the three-point interactions. The dynamic loop involves the chiral α-carbon of an external guest to generate a chiral environment around the N-terminal segment, in turn leading to the predominant formation of a one-handed helix for the following achiral residues.

According to a 3_{10}-helical hydrogen-bonding scheme (Figure 2), the two amide NH's from the N-terminus are invariably present as "free hand". In 3_{10}-helical oligopeptides in the crystalline state, these two NH's are often found to participate in hydrogen bonding to a cocrystallized solvent molecule and/or to two free carbonyl groups around the C-terminus of a neighboring peptide molecule.[13g,16c−f,h,i,k−o,s,u,17c] Such a head-to-tail hydrogen-bonding fashion forms a continuous helical column. On the other hand, our present findings explicitly demonstrate that the two "free hands" always located at the N-terminus of a 3_{10}-helix, even in solution, play a significant role for dynamic chiral recognition of an external molecule involving at least both carboxyl and urethane groups.

It was qualitatively suggested that the terminus of α-helical polypeptides possesses "chirality".[36] Meanwhile, our present result proves that a 3_{10}-helix possesses intrinsically a chiral recognition site on its N-terminal backbone. Furthermore, external chiral signal acquired therein should transfer to the other terminus to influence the original helicity.

Low-Temperature NMR and NOESY Studies. Figure 12 shows the temperature dependence of ^{1}H NMR spectra of peptide **1** with an excess of Boc-L-Leu-OH (6.4-fold).

The most striking feature at a lower temperature is the unequivalent splitting of an NH resonance; for example, Δ^ZPhe(2) NH far downfield (10.1 ppm) becomes sharper, while small resonances appear at 9.7 and 8.85 ppm concomitantly. The Δ^ZPhe(2) NH peak at 10.1 ppm, although somewhat smaller than a single proton, adds to the peak at 9.7 ppm or at 8.85 ppm to make the integral of a single proton. Thus, either of these small peaks should be assigned to the satellite peak of the Δ^ZPhe(2) NH resonance. This tentative assignment could be confirmed by the corresponding NOESY spectrum at 268 K (Figure 13), which gave a strong NOE between peaks of 10.1 and 9.7 ppm, both of which are assignable to chemical exchange of the identical proton.

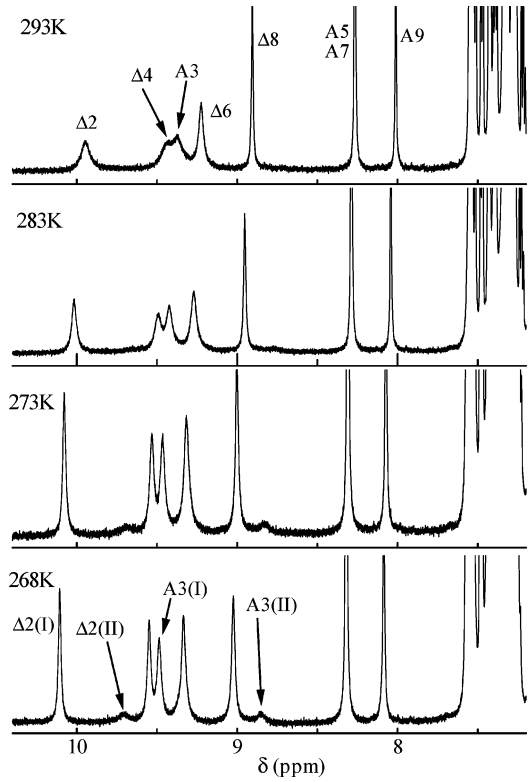

Figure 12. Expanded 600 MHz ^{1}H NMR spectra (NH and aromatic regions) of peptide **1** with Boc-L-Leu-OH in $CDCl_3$ at (a) 293 K, (b) 283 K, (c) 273 K, and (d) 268 K: [**1**] = 1.9 mM and [Boc-L-Leu-OH] = 12.2 mM. Δ and A denote Δ^ZPhe and Aib, respectively, and the number after Δ or A is the residue number from the N-terminus. (I) and (II) also represent the corresponding main and satellite peaks, respectively.

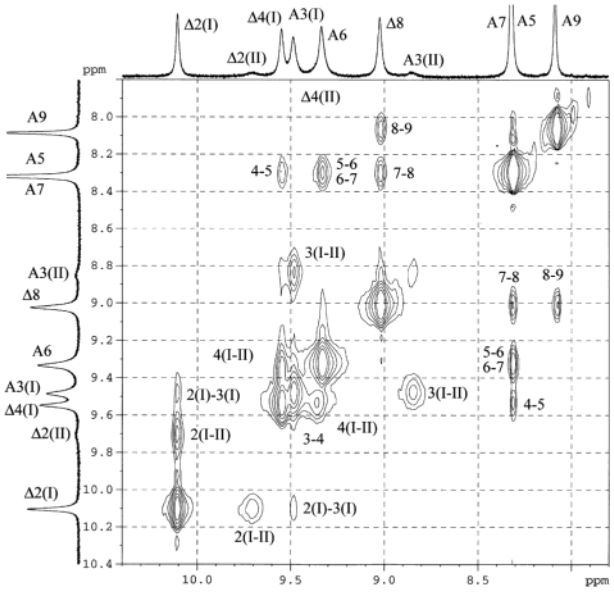

Figure 13. Expanded NOESY spectrum (NH regions) of peptide **1** with Boc-L-Leu-OH in $CDCl_3$ at 268 K; [**1**] = 1.9 mM and [Boc-L-Leu-OH] = 12.2 mM. Δ and A denote Δ^ZPhe and Aib, respectively, and the number after Δ or A is the residue number from the N-terminus. (I) and (II) represent the corresponding main and satellite peaks, respectively.

In addition, two satellite peaks were specified at 9.4 ppm for Δ^ZPhe(4) NH and at 8.85 ppm for Aib(3) NH. The biased split of Δ^ZPhe(2)−Δ^ZPhe(4) NH resonances should not be based on Boc-amino acid-bound peptide versus isolate peptide. Rather it might be attributed to a conformational transition between two

(36) Induced CD signals were observed for CT complex generated by head-to-tail dimerization of one-handed α-helical polypeptides. For the details, see: Shimizu, T.; Sisido, Y.; Imanishi, Y. *Biopolymers* **1980**, *19*, 1271−1279.

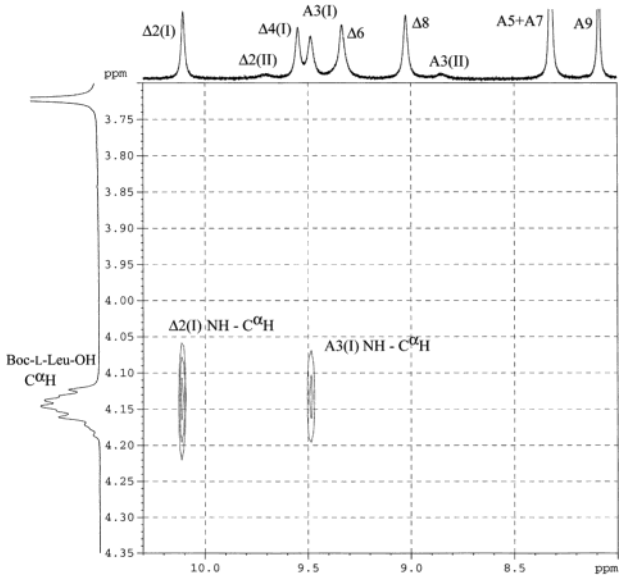

Figure 14. Expanded NOESY spectrum [regions between NH's (peptide **1**) and $C^{\alpha}H$ (Boc-L-Leu-OH)] in the same chart as Figure 13.

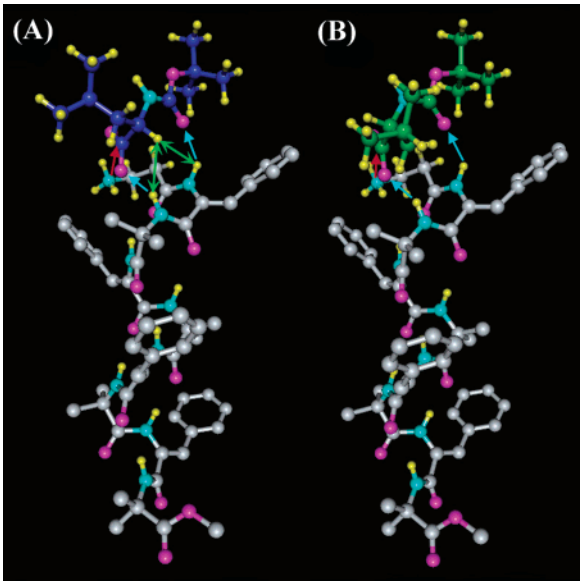

Figure 15. Energy-minimized complex of a right-handed 3_{10}-helical peptide **1** with (A) Boc-L-Leu-OH (blue bond) or (B) Boc-D-Leu-OH (green bond). The minimization was performed by semiempirical MO calculation (AM1 method in MOPAC97).[21] In both figures, all peptide protons other than NH's and β-Ala are omitted for clarification. The total energy of complex A was lower by 3.14 kcal mol^{-1} than that of complex B. The blue arrows represent two hydrogen bonds between peptide **1** and Boc-Leu-OH, that is, Aib(3) NH versus carboxylate oxygen, and Δ^{Z}Phe(2) NH versus urethane carbonyl oxygen. The red one stands for the ionic interaction of β-Ala(1) ammonium with the carboxylate of Boc-Leu-OH. In (A), the green arrows also indicate the proton pairs that led to the marked NOEs (as shown in Figure 14).

dissimilar forms in complexation, for example, the induced right-handed helix versus left-handed helix, because the complexation is judged to be almost complete from the NMR concentration and the binding constant estimated from the CD titration. Under this assumption, the main peak (I) might correspond to a right-handed helix induced by Boc-L-Leu-OH, whereas the satellite (II) might correspond to a left-handed one. From the integral ratio of the (I) peak to the corresponding (II) peak, we here can estimate 87/13 for the molar ratio of right-handed/left-handed helices at 268 K. Consequently, the chiral stimulus to a 3_{10}-helix terminus enables the optically inactive backbone to induce a predominant bias toward a one-handed helix. In Figure 13, marked NOEs were observed for $N_iH-N_{i+1}H$ pairs of the segment of Δ^{Z}Phe(2)−Aib(9), as found in peptide **1** alone.[18] This means that a helical conformation of peptide **1** alone is maintained in the complexation process.

In the same NOESY spectrum (Figure 14), there exist two marked cross-peaks between peptide **1** and Boc-L-Leu-OH: $C^{\alpha}H$ (Boc-L-Leu-OH) versus the main peak of Δ^{Z}Phe(2) NH, and $C^{\alpha}H$ (Boc-L-Leu-OH) versus the main peak of Aib(3) NH, while no other cross-peaks between the two species were found.

Similar tendency was observed in the NOESY spectrum of peptide **1** with Boc-L-Pro-OH at 268 K in $CDCl_3$. Obviously, the dynamic complex leading to a right-handed helix requires the proximities of the above two proton pairs. This structural information directly proves the NCDE that literally starts from the N-terminal segment "bitten" by a chiral guest, but not from the remaining residues of the 3_{10}-helix.

Theoretical Estimation of Chiral Complex Structure. The preceding CD and NMR results propose the dynamic complex depicted in Figure 11. The most likely question raised at this point is whether the proposed complex is energetically permitted to form, and, furthermore, why Boc-L-amino acid chooses the induction of a right-handed helix. For the clarification of these points, the semiempirical MO calculation (AM1 method in MOPAC97)[21] was applied to the present system. Modeling of an initial structure for searching a stable Boc-L-Leu-OH-bound peptide was performed on the basis of Figure 11. This procedure should be valid, because the computation aims at the theoretical verification of the experimentally proposed complex, but not at global searching of the lowest-energy one.

According to Figure 11, the β-Ala residue needs to take a bend conformation to enable the N-terminal amino group to approach the Aib(3) NH, whereas the β-Ala residue in the lowest-energy structure of peptide **1** (Figure 4) prefers a semi-extended conformation characterized by θ ($N-C^{\beta}-C^{\alpha}-C'$) = −173° and ψ ($C^{\beta}-C^{\alpha}-C'-N$) = −70°. Thus, in the first step, such a bend conformation was produced from Figure 4 (the right-handed helix) only through the alternation in the θ and ψ angles (θ = 66° and ψ = −175°), which might be energetically permitted due to a high flexibility inherent in the β-Ala main chain.[15] Subsequently, a Boc-L-Leu-OH molecule was placed at the N-terminal segment of the right-handed helix through the three-point coordination proposed in Figure 11, including the salt bridge formation of $-COO^{-}\cdot NH_3^{+}-$. The energy minimization from the initial structure was carried out with all bond lengths, bond angles, and dihedral angles, while only the three N−H bond lengths of the ammonium terminus were fixed to 1.0 Å to conserve the salt bridge during the minimization course.

The converged structure, as shown in Figure 15A, retains substantially the initial conformation.

Herein, the two intermolecular hydrogen bonds are maintained with the following parameters: d (H···O) = 2.07 Å and ∠N−H···O = 150° for Aib(3) NH versus carboxylate oxygen of Boc-L-Leu-OH; d (H···O) = 2.2 Å and ∠N−H···O = 136° for Δ^{Z}Phe(2) NH versus urethane carbonyl oxygen of Boc-L-Leu-OH. In addition, the theoretical structure is fully supported by the intermolecular NOEs in the preceding section. That is, the theoretical complexation is accompanied with the proximities

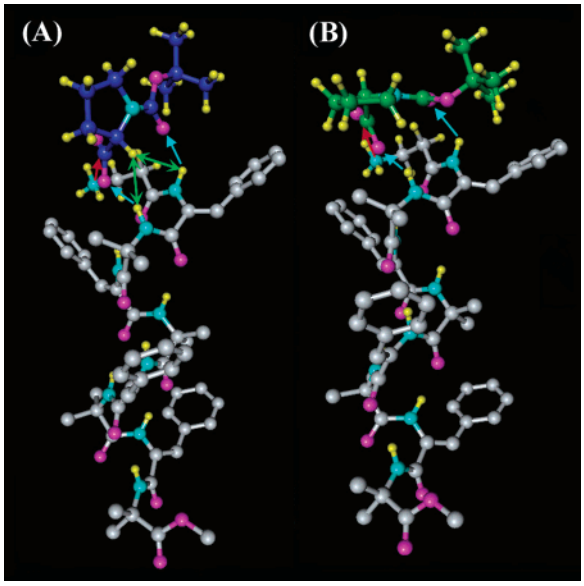

Figure 16. Energy-minimized complex of a right-handed 3_{10}-helical peptide **1** with (A) Boc-L-Pro-OH (blue bond) or (B) Boc-D-Pro-OH (green bond). The total energy of complex A was lower by 3.3 kcal mol^{-1} than that of complex B. For an explanation of the arrows, refer to the caption of Figure 15.

of Boc-L-Leu-OH C$^{\alpha}$H to Δ^{Z}Phe(2) NH (3.3 Å) or to Aib(3) NH (2.6 Å), both of which in fact exhibited the marked NOE signals (Figure 14). In contrast, the other interproton distances between the two species are considerably large, for example, Boc-L-Leu-OH C$^{\alpha}$H to β-Ala(2) C$^{\alpha}$H$_2$ (4.3 Å for average of both C$^{\alpha}$H$_2$ protons), and to β-Ala(2) C$^{\beta}$H$_2$ (6.0 Å), in both of which the NOE signals were not observed reasonably. A similar theoretical structure was obtained for the Boc-L-Pro-OH-bound peptide molecule (Figure 16A), in which the interactive sites are composed of the salt bridge ($-COO^{-}\cdot NH_3^{+}-$) and the two hydrogen bonds of the Δ^{Z}Phe(2) NH → urethane C=O of Boc-Pro-OH and of the Aib(3) NH → O atom of COO^{-}. In the theoretical complex, smaller interproton distances are expected only for Boc-L-Pro-OH C$^{\alpha}$H to Δ^{Z}Phe(2) NH (3.7 Å) or to Aib-(3) NH (2.6 Å), similar to the case of Boc-L-Leu-OH. These proton pairs in fact exhibited marked NOE signals, as mentioned in the preceding section.

Therefore, it has been demonstrated experimentally and theoretically that the 3_{10}-helix is able to capture a Boc-amino acid molecule on the N-terminal segment involving the two free amide NH's. It should be noted that the 3_{10}-helical structures of -(Δ^{Z}Phe-Aib)$_4$-OMe in the complex and peptide **1** alone are almost the same.[37] This implies that only a minor conformational change in the flexible N-terminal β-Ala is required for the binding of a Boc-amino acid molecule, whereas the original positions of the two free amide NH's are essentially retained in the complexation state. These free NH's, parallel to the helical axis, are directed to a free space around the N-terminus, thereby enabling effective binding of a chiral guest. As is frequently found in the crystal structures of 3_{10}-helical peptides, such N-terminal free NH's are prone to form a hydrogen bond to neighboring molecules. Thus, the N-terminal complexation mediated by intermolecular hydrogen bonding originates from a general function inherent in natural 3_{10}-helical segments, but not from special phenomenon driven from our unusual sequence.

(37) See the Supporting Information.

Next, we proceed to consider the second important issue as to why a Boc-L-amino acid molecule chooses preferentially a right-handed helix, not a left-handed helix. For clarification, energy minimization was performed for a complex of Boc-D-Leu-OH and a right-handed 3_{10}-helix. In the initial conformation, only the C$^{\alpha}$H proton and isobutyl side chain within Boc-L-Leu-OH in Figure 15A were exchanged to produce Boc-D-Leu-OH under the conservation of the three-point interactions. The energy-minimized structure is shown in Figure 15B. The total energy was higher by 3.14 kcal mol^{-1} than that in Figure 15A, strongly indicating that a combination of Boc-L-Leu-OH and the right-handed helix is energetically more stable than that of Boc-D-Leu-OH and the right-handed helix (or Boc-L-Leu-OH and the left-handed helix). The energy difference should arise from a different manner in steric interactions between the side chain of Boc-Leu-OH and the N-terminal segment. The isobutyl side chain of Boc-D-Leu-OH approaches the Δ^{Z}Phe(2) residue in the right-handed 3_{10}-helix, particularly its styryl moiety, thereby leading to unfavorable steric repulsion between both species. In contrast, such structural distortion can be fully relaxed in the case of Boc-L-Leu-OH (Figure 15A), in which the side chain is directed toward a free space opposite to the Δ^{Z}Phe(2) residue.

A similar tendency was seen in the case of Boc-Pro-OH, where the complex of the L-isomer and a right-handed helix (Figure 16A) was more stable by 3.3 kcal mol^{-1} than that of the D-isomer and a right-handed helix (Figure 16B). The unstable complexation for Boc-D-Pro-OH is mainly based on the steric repulsion between the Boc group and Δ^{Z}Phe(2) residue. In contrast, in the case of the L-form, the Boc group as well as its pyrrolidine ring is placed at a position remote from the Δ^{Z}Phe(2) residue, while the complex is keeping the three-point interactions proposed in Figure 11. The similar chiral induction mechanism should be applicable to the other Boc-L-amino acids or peptide acid (*S*)-**7**, all of which induce the same right-handed helix.

Concluding Remarks

We here have proposed novel chiral interactions applicable to 3_{10}-helical segments ubiquitous in natural peptides and proteins. In biological systems, chiral recognition and reaction often occur in an asymmetric spatial array of functional side chains on a ternary protein backbone. On the other hand, it is not so clear whether chiral recognition potency is involved in a helical peptide backbone itself. The clarification of the NCDE mechanism demonstrates that a 3_{10}-helix possesses intrinsically a chiral recognition site at its N-terminal segment including the two free amide NH's, which always appear from the hydrogen-bonding mode. These two NH's are cooperatively hydrogen-bonded to a Boc-L-amino acid (or peptide acid) molecule to generate a chiral looping complex that is capable of influencing the original chiral structure of the entire chain.

In the last two decades, special attention has been paid to the significance of the terminal sequence of natural α-helical segments in proteins and peptides.[38] In particular, the first (N-terminal) and last (C-terminal) four residues lacking intramolecular hydrogen-bonding partners, defined as "helix-capping", play a vital role for the enhancement of structural stability of an entire α-helix. The above insightful, statistical and experimental analyses of natural helical sequences have indicated that several residues such as Asn, Ser, Asp, Gly, and Thr are

preferred at the N-cap position (N-terminus). The significance of these N-cap residues other than Gly is addressed to the side-chain functionality that is prone to form a hydrogen bond to free amide NH of the N-capping sequence (third or second amide from the N-cap). Such a hydrogen bond between the side chain and main chain was sometimes mediated by a solvent molecule to form a bridge.[38e] In addition, a reciprocal hydrogen bond is often accompanied between N-cap NH and the other residue's side chain to create an "N-capping box".[39]

According to these elegant principles, N-terminal free amide groups are very "interactive" and thus eager to seek hydrogen-bond accepting partners. In this regard, our looping complexation on the two free NH's should originate from the nature of the "N-capping 3_{10}-helical sequence". Furthermore, our present findings newly appeal that the N-capping backbone itself (more precisely, the spatial array of the two free NH's) is capable of recognizing the chirality of an external peptide molecule, subsequently converting the acquired chiral sign and power into a dynamic control of the original helicity and helical stability. Our current efforts are directed toward the application of the NCDE to aqueous solution or to oligopeptides containing natural chiral residues in the N-capping sequence, to generalize the novel biological interaction in peptide and protein science.

Experimental Section

Materials. All amino acids and coupling reagents were purchased from Tokyo Kasei Co. (Tokyo, Japan) or Kokusan Chemical Works Ltd. (Tokyo, Japan). Boc-amino acid was prepared by a standard procedure[40] with $(Boc)_2O$ or was purchased from Kokusan Chemical Works Ltd. Butyryl-L-Leu-OH was prepared by coupling butyric acid and Leu via a standard mixed anhydride method.[40] (*S*)-(+)-α-Phenylethylamine was purchased from Tokyo Kasei Co., (*S*)-(+)-2-phenylpropionic acid was purchased from ACROS Organics (NJ), and the other chiral reagents were purchased from Aldrich Co. (WI). Chloroform dried over $CaSO_4$ was distilled onto $CaSO_4$ before use. *N*,*N*-Dimethylformamide (DMF) was purified by distillation with ninhydrin under a reduced pressure. Thin-layer chromatography (TLC) was performed on precoated silica plates in the following solvent systems: (A) ethyl acetate, (B) methanol, (C) chloroform−methanol (9:1), and (D) 1-butanol−acetic acid−water (7:2:1). A single spot in the TLC was obtained for each of the final products and their intermediates, as indicated below.

Boc-β-Ala-Δ^ZPhe Azlactone. The azlactone was prepared from Boc-β-Ala-DL-phenyl serine according to ref 24e,f. mp 120.5−122 °C. $R_f^A = 0.76$; $R_f^B = 0.88$; $R_f^C = 0.85$; $R_f^D = 0.96$. 200 MHz ^{1}H NMR (δ, in $CDCl_3$): 8.10−8.05 + 7.47−7.44 (2H + 3H, m, phenyl H Δ^ZPhe), 7.18 (1H, s, C$^\beta$H Δ^ZPhe), 5.15−5.05 (1H, m, NH β-Ala), 3.67−3.58 (2H, m, C$^\beta$H$_2$ β-Ala), 2.91−2.85 (2H, m, C$^\alpha$H$_2$ β-Ala), and 1.44 (9H, s, 3 × CH_3 Boc). FT-IR (cm^{-1}, in KBr): 3363, 1789, 1688, 1662, 1608, 1537.

Boc-β-Ala-(Δ^ZPhe-Aib)$_4$-OMe. Boc-β-Ala-Δ^ZPhe azlactone (2.32 g, 7.3 mmol) and H-(Aib-Δ^ZPhe)$_3$-Aib-OMe[13j] (5.17 g, 6.4 mmol) were dissolved in DMF (40 mL) at room temperature, and the mixture was stirred for 96 h. After the reaction mixture was concentrated in vacuo, the residue was washed with chloroform and subsequently crystallized from the methanol solution by slow evaporation at room temperature. Yield: 4.8 g (66.7%). mp 270−271 °C. $R_f^A = 0.51$; $R_f^B = 0.95$; $R_f^C = 0.39$; $R_f^D = 0.94$. 600 MHz ^{1}H NMR [δ, in $CDCl_3$ containing 17 vol % $(CD_3)_2SO$]: 9.87 [1H, s, NH Δ^ZPhe(2)], 9.40 [1H, s, NH Δ^ZPhe(4)], 9.19 [1H, s, NH Δ^ZPhe(6)], 8.82 [1H, s, NH Δ^ZPhe(8)], 8.60 [1H, s, NH Aib(3)], 8.33 [1H, s, NH Aib(7)], 8.28 [1H, s, NH Aib(5)], 7.95 [1H, s, NH Aib(9)], 7.59−6.81 [24H, m, 4 × (phenyl H + C$^\beta$H) Δ^ZPhe], 5.69 [1H, bs, NH β-Ala(1)], 3.68 (3H, s, $COOCH_3$), 3.11 (2H, bs, C$^\beta$H$_2$ β-Ala), 2.47 (2H, bs, C$^\alpha$H$_2$ β-Ala), 1.62 + 1.56 + 1.52 + 1.35 (24H, s + s + s + s, 8 × CH_3 Aib), and 1.45 (9H, s, 3 × CH_3 Boc). FT-IR (cm^{-1}, in KBr): 3262, 1715, 1658, 1629, 1539.

H-β-Ala-(Δ^ZPhe-Aib)$_4$-OMe (1). Boc-β-Ala-(Δ^ZPhe-Aib)$_4$-OMe (500 mg, 0.44 mmol) was dissolved in formic acid, and the solution stood for 18 h at room temperature. After concentration in vacuo, 5% $NaHCO_3$ solution was added to the residue, which was subsequently extracted with chloroform. The organic layer was washed with 5% $NaHCO_3$ solution and was dried over $MgSO_4$. The product was obtained by precipitation from chloroform/methyl acetate. Yield: 255 mg (56%). mp 254−256 °C. $R_f^A = 0$; $R_f^B = 0.22-0.33$; $R_f^C = 0$; $R_f^D = 0.57-0.64$. 600 MHz ^{1}H NMR (δ, in $CDCl_3$): 9.25 [1H, s, NH Δ^ZPhe(4)], 9.16 [1H, s, NH Δ^ZPhe(6)], 8.91 [1H, s, NH Δ^ZPhe(8)], 8.28 [1H, s, NH Aib(3)], 8.24 [1H, s, NH Aib(7)], 8.12 [1H, s, NH Aib(5)], 7.99 [1H, s, NH Aib(9)], 7.53−7.21 + 6.92 [24H, m + s, 4 × (phenyl H + C$^\beta$H) Δ^ZPhe], 3.63 (3H, s, $COOCH_3$), 2.82 (2H, bs, C$^\beta$H$_2$ β-Ala), 2.33 (2H, bs, C$^\alpha$H$_2$ β-Ala), 1.57 + 1.55 + 1.53 + 1.29 (24H, bs + s + s + bs, 8 × CH_3 Aib). FT-IR (cm^{-1}, in KBr): 3273, 1739, 1657, 1623, 1536. MS (MALDI-TOF) (*m*/*z*), $[M + Na]^+$ (calcd = 1047.160): found 1047.15.[41]

Spectroscopic Measurements. ^{1}H NMR spectra were recorded on Bruker DRX-600 (600 MHz) or DPX-200 (200 MHz) spectrometers at 293 K for peptide **1** (1−2 mM) in $CDCl_3$. All chemical shifts in ppm were determined using tetramethylsilane as an internal standard. NOESY spectra were measured on the Bruker DRX-600 using a Bruker standard pulse program (noesytp)[42] with a mixing time of 200 ms, 8 transients per t_1, 2 K data points in the t_2 domain, and 256 points in the t_1 domain. The data processing and analysis were performed with the XWINNMR software (version 2.5). FT-IR spectra for peptide **1** were recorded on a JASCO FT/IR-430 spectrometer in KBr and in chloroform. CD and UV spectra were recorded at ambient temperature (ca. 293 K) for a chloroform solution of peptide (0.14 mM) containing various amounts of carboxylic acid (0−150 mM) on JASCO J-600 and JASCO V-550 spectrometers, respectively. A quartz cell of 1 mm-optical path length was used. Chloroform for the solvent was purified by distillation over $CaSO_4$ before use. The peptide concentration was determined on the basis of $\epsilon_{280} = 1.8 \times 10^4$ per Δ^ZPhe residue. The MALDI-TOF mass spectrum of the final peptide was acquired on PerSpective Biosystems Voyager RP in reflectron mode, using 1,8-dihydroxy-9(10*H*)-anthracenone (1,8,9-anthracenetriol) matrix and NaI salt for the sample preparation.

(38) (a) Presta, L. G.; Rose, G. D. *Science* **1988**, *240*, 1632−1641. (b) Richardson, J. S.; Richardson, D. C. *Science* **1988**, *240*, 1648−1652. (c) Serrano, L.; Fersht, A. R. *Nature* **1989**, *342*, 296−299. (d) Doig, A. J.; Baldwin, R. L. *Protein Sci.* **1995**, *4*, 1325−1336. (e) Thanki, N.; Umrania, Y.; Thornton, J. M.; Goodfellow, J. M. *J. Mol. Biol.* **1991**, *221*, 669−691. (f) Chen, Y. W.; Fersht, A. R. *FEBS Lett.* **1994**, *347*, 304−309. (g) Cochran, D. A. E.; Penel, S.; Doig, A. J. *Protein Sci.* **2001**, *10*, 463−470. (h) Wilson, C. L.; Hubbard, S. J.; Doig, A. J. *Protein Eng.* **2002**, *15*, 545−554. (i) Cochran, D. A. E.; Doig, A. J. *Protein Sci.* **2001**, *10*, 1305−1311. (j) Doig, A. J.; Macarthur, M. W.; Stapley, B. J.; Thornton, J. M. *Protein Sci.* **1997**, *6*, 147−155. (k) Aurora, R.; Srinivasan, R.; Rose, G. D. *Science* **1994**, *264*, 1126−1130. (l) Chakrabartty, A.; Doig, A. J.; Baldwin, R. L. *Proc. Natl. Acad. Sci. U.S.A.* **1993**, *90*, 11332−11336. (m) Petukhov, M.; Muñoz, V.; Yumoto, N.; Yoshikawa, S.; Serrano, L. *J. Mol. Biol.* **1998**, *278*, 279−289. (n) Petukhov, M.; Uegaki, K.; Yumoto, N.; Yoshikawa, S.; Serrano, L. *Peptide Sci.* **1999**, *8*, 2144−2150. (o) Baldwin, R. L.; Rose, G. D. *Trends Biochem. Sci.* **1999**, *24*, 26−33.

(39) (a) Harper, E. T.; Rose, G. D. *Biochemistry* **1993**, *32*, 7605−7609. (b) Lyu, P. C.; Wemmer, D. E.; Zhou, H. X.; Pinker, R. J.; Kallenbach, N. R. *Biochemistry* **1993**, *32*, 421−425. (c) Seale, J. W.; Srinivasan, R.; Rose, G. D. *Protein Sci.* **1994**, *3*, 1741−1745. (d) Zhou, H. X.; Lyu, P.; Wemmer, D. E.; Kallenbach, N. R. *Proteins* **1994**, *18*, 1−7.

(40) For a review of procedures of peptide synthesis, see: Izumiya, N.; Kato, T.; Aoyagi, H.; Waki, M. *Principle and Practice of Peptide Synthesis. (Pepuchido Gosei no Kiso to Jikken)*; Maruzen Co., Ltd.: Tokyo, Japan, 1985.

(41) MALDI-TOF mass was measured for HCOOH·peptide **1**, of which the formic acid was completely dissociated from the peptide in the ionization course. The spectrum thus showed a single peak excepted for $[M + Na]^+$: see the Supporting Information.

(42) Bodenhausen, G.; Kogler, H.; Ernst, R. R. *J. Magn. Res.* **1984**, *58*, 370−388.

Conformational Energy Calculation. The energy-minimized conformation of peptide **1** alone was obtained using the semiempirical MO calculation (AM1 method in MOPAC97).[21] The initial conformation was generated from the modified PEPCON,[43] where the -Δ^ZPhe-(Aib-Δ^ZPhe)$_3$- was set to a standard right-handed 3_{10}-helix ($\phi = -60°$, $\psi = -30°$, and $\omega = 180°$)[44] on the basis of the experimental data. The C-terminal Aib(9) took the opposite handedness ($\phi = 60°$, $\psi = 30°$, and $\omega = 180°$), because the helix inversion at the C-terminus was often found in analogous peptides[17c] and Aib-containing peptides.[13d,16c−e,i] The β-Ala residue was set to a fully extended conformation of $\theta = 180°$ and $\psi = 180°$. The minimization with a MOPAC97 keyword of MMOK, which corrects the rotational barrier about amide bonds, was carried out for the variables of all bond lengths, bond angles, and torsion angles. An INDO/S-SCI calculation was performed using MOS-F[24i] in WinMOPAC.[45] The molecular graphics were illustrated using the molecular modeling softwares.[46]

Acknowledgment. This work was supported by the Ministry of Education, Culture, Sports, Science, and Technology of Japan under a grant to Y.I. The authors wish to express their sincere gratitude to Professor M. Kawai in the Department of Applied Chemistry, Nagoya Institute of Technology, for the use of his CD apparatus. We also thank M. Eng. Y. Ookouchi for technical assistance.

Note Added after ASAP. The values of the β-Ala's θ and ψ angles were incorrect in the version published on the Web on 6/12/2003. The values in the version published 6/13/2003 and in the print version are correct.

Supporting Information Available: Location of Δ^ZPhe transition moments around 280 nm in a right-handed 3_{10}-helical peptide **1**, Job plot of induced CD amplitude, structural comparison between Boc-L-Leu-OH-bound peptide **1** and peptide **1** alone, and MALDI-TOF mass spectrum (PDF). This material is available free of charge via the Internet at http://pubs.acs.org.

JA035040S

(43) For the original PEPCON, see: (a) Momany, F. A.; McGuire, R. F.; Burgess, A. W.; Scheraga, H. A. *J. Phys. Chem.* **1975**, *79*, 2361−2381. (b) Beppu, Y. *Comput. Chem.* **1989**, *13*, 101. (c) Sisido, M. *Pept. Chem.* **1992**, *1991*, 105−110. For the modified version for dehydroarylalanine-containing peptides, see: (d) Inai, Y.; Kurashima, S.; Hirabayashi, T.; Yokota, K. *Biopolymers* **2000**, *53*, 484−496. (e) Inai, Y.; Oshikawa, T.; Yamashita, M.; Hirabayashi, T.; Hirako, T. *Biopolymers* **2001**, *58*, 9−19. (f) Inai, Y.; Hirabayashi, T. *Biopolymers* **2001**, *59*, 356−369. (g) Inai, Y.; Oshikawa, T.; Yamashita, M.; Hirabayashi, T.; Kurokawa, Y. *Bull. Chem. Soc. Jpn.* **2001**, *74*, 959−966.

(44) (a) Paterson, Y.; Rumsey, S. M.; Benedetti, E.; Nemethy, G.; Scheraga, H. A. *J. Am. Chem. Soc.* **1981**, *103*, 2947−2955. (b) Ramachandran, G. N.; Sasisekharan, V. *Adv. Protein Chem.* **1968**, *23*, 283−437.

(45) WinMOPAC V2.0; Fujitsu Ltd., Tokyo, Japan, 1998.

(46) Butch Software Studio, *FREE WHEEL for Windows: 0.60E* for Molecular Modeling Software, Japan, 2001; Butch Software Studio, *MIDZUKI: 0.30*, Japan, 2001.